2011 14th International IEEE Conference on
Intelligent Transportation Systems
Washington, DC, USA. October 5-7, 2011

Arterial Travel Time Estimation Based On Vehicle Re-Identification Using Magnetic Sensors: Performance Analysis

Rene O. Sanchez*, Christopher Flores†, Roberto Horowitz*, Ram Rajagopal‡ and Pravin Varaiya†
*Department of Mechanical Engineering
University of California, Berkeley, CA 94720, US
Emails: r2sanche@me.berkeley.edu and horowitz@me.berkeley.edu
†Sensys Networks, Inc, Berkeley, CA 94710, US
Emails: chrisf@sensysnetworks.com and pvaraiya@sensysnetworks.com
‡Department of Civil and Environmental Engineering
Stanford University, Stanford, CA 94305, US. Email: ram.rajagopal@stanford.edu

***Abstract*—Two versions of an arterial travel time estimation method based on vehicle re-identification using wireless magnetic sensors were studied across an arterial segment with multiple intersections. Both methods are based on the same travel time estimation system, but one of them uses the so called *original* signal processing algorithm while the other one uses a recently *modified* version of it. Both methods were tested on a 0.51 km (0.32 mile)-long segment of West 34th Street in New York, NY, under harsh driving conditions (i.e. right after a winter storm). The original and modified system results were compared against ground truth data obtained from video. Based on the ground truth data it was possible to determine the travel time distribution and the percentage of vehicles that each of the different methods was able to re-identify. During an analysis period of 45 minutes, 318 vehicles were registered to go across the arterial segment. The original method has a 62% re-identification rate, while the modified method has a 69% rate. Based on comparisons of travel time distribution and empirical cumulative distribution functions, it was observed that the modified method travel time distribution is closely related to the ground truth distribution, while the original method significantly diverges from the ground truth at long travel times.**

Keywords: Vehicle Re-Identification; Real-Time Travel Time Estimation; Arterial Performance Measures; Magnetic Signature

I. INTRODUCTION

The work presented in this paper is a continuation of the work in [1], where the vehicle re-identification algorithm used in the arterial travel time estimation system, discussed in [2] and considered for this analysis, was revised, improved and validated at a single lane loop on-ramp. The modified vehicle re-identification algorithm that resulted from [1] showed an improved vehicle re-identification rate and accuracy at the test site.

In heavily used arterial streets, where stop-and-go traffic is similar to the one observed in on-ramps under congested conditions, the modified vehicle re-identification algorithm explained in [1] has the potential to improve travel time estimation. In order to determine the effect of the modified method on arterial travel time estimation, a field test was performed in a segment of West 34th Street in New York City (Figure 1). The performance of the original system and the system with the modified vehicle re-identification algorithm is studied using ground truth data obtained from video.

The paper is organized as follows: the arterial travel time estimation system is summarized in Section II. The test site and vehicle detection installation are described in Section III. The ground truth (GT) and the magnetic sensor array data are explained in Section IV. An analysis of the ground truth and the vehicle detection system data is presented in Section V. Section VI contains the results of the arterial travel time estimation methods and the performance analysis of both methods based on ground truth. Conclusions are presented in Section VII.

II. ARTERIAL TRAVEL TIME ESTIMATION SYSTEM

The system relies on matching vehicle signatures from wireless sensors. The sensors provide a magnetic signature of a vehicle and the time when the magnetic signature is measured. A re-identification of signatures between two locations gives the corresponding travel time of the vehicle. The travel times for all matched vehicles yield the travel time distribution. The travel time estimation method summarized in this section is described in [2].

A. Vehicle Magnetic Signature

The magnetic vehicle signature consists of a collection of peak value sequences (local maxima and minima) extracted from the 'raw' magnetic signals measured by an array of sensors. Each sensor has a three-axis magnetometer that measures the *x, y and z* directions of the earth's magnetic field as a vehicle goes over it. Each sensor generates three peak sequences extracted from the x, y and z component signals, which constitute a signature slice $X^i = (X^i_x, X^i_y, X^i_z)$. For this analysis, five slices constitute a vehicle's signature, since there are five sensors in each array.

B. Vehicle Re-Identification Algorithm Summary

The vehicle re-identification is done in two steps:

1) Signal Processing Step: In this step, each pair (X_i, Y_j) of start and end vehicle signatures is compared to produce a distance $d(i,j) = \delta(X_i, Y_j) \geq 0$ between them. The smaller $\delta(X_i, Y_j)$ the more likely it is that X_i, Y_j are signatures of the same vehicle. This step reduces the two signature arrays $X =$

$\{X_i, i = 1, \cdots, N\}$ and $Y = \{Y_j, j = 1, \cdots, M\}$ to the $N \times M$ distance matrix $D = \{d(i, j) \mid 1 \leq i \leq N, 1 \leq j \leq M\}$.

This step of the vehicle re-identification method was modified in [1] in order to enhance the matching rate and accuracy during congested conditions, when vehicles travel slowly or stop while going over the array of sensors. For this analysis, *original method* refers to the arterial travel time estimation system as described in [2], while *modified method* refers to the same system with the enhanced signal processing step described in [1].

2) Matching Step: In the second step a *matching function* assigns to each distance matrix D a matching $\mu : \{1, \ldots, N\} \to \{1, \ldots, M, \tau\}$, with the following interpretation: $\mu(i) = j$ means that the start (upstream) vehicle i is declared to match (be the same as) end (downstream) vehicle j; $\mu(i) = \tau$ means i is declared not to match any downstream vehicle.

In this step, a constrained matching function is used, which does not permit vehicle overtaking. The algorithm matches the largest number of vehicles that satisfy the First In, First Out (FIFO) condition. Note that this constraint slightly affects the matching rate (e.g. less potential vehicles available to re-identify) but greatly improves accuracy if vehicle overtaking is not significant [2].

C. Travel Time Estimation

Every time a vehicle signature is measured, a corresponding time stamp is paired to the signature. The start and end sensor array data correspond to a collection of data pairs of the form (s_i, X_i) and (t_j, Y_j), respectively. When two signatures (X_i, Y_j) are determined to be a match by the vehicle re-identification algorithm, the travel time across the segment is determined to be $t_j - s_i$.

In a deployment like the one shown in Figure 1, where the arterial segment is composed of multiple lanes, the vehicle re-identification algorithm is traditionally used with upstream and downstream array data coming from the same lane. For the NY test site, the traditional way to run the algorithm would involve using data from the fast lane start and end arrays, represented by $fast \to fast$, independently of the data coming from the slow lane start and end arrays, depicted by $slow \to slow$. This practice is based on the assumption that for the most part, vehicles tend to stay in their same lane as they go through the segment.

III. TEST SITE

The New York City arterial test site is a 0.51 km (0.32 mile)-long segment of West 34th Street that intersects the 7th and 8th avenue (see Figure 1). The segment is formed by three lanes, however, this analysis focuses on the travel time estimation of vehicles in the fast and slow lanes. The third one, a bus only lane, was not transited during the analysis period because it was blocked at different locations along the segment as shown in Figure 2 (b).

This test site is a suitable location to study the performance of arterial travel time estimation systems, since it has a

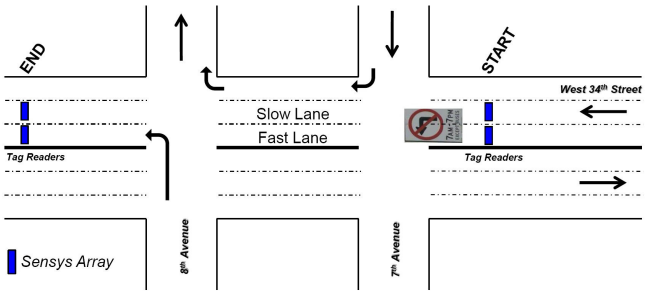

Fig. 1. 0.32-mile segment of 34th Street in New York City

configuration and driving dynamics that encompasses what can be encountered in arterial streets in many big cities: drivers are aggressive, lane changing is significant, taxis and buses stop as they go across the segment, people double park, and there is vehicle queueing at the detector locations. Furthermore, vehicles get in and out of the segment not only at the start and end locations, but also at the intersections in between. If a travel time estimation system yields accurate results under these traffic conditions, then it can be expected to have a comparable or better performance in arterial streets where traffic conditions are more ordered and less congested.

The locations of the sensor arrays at this test site do not follow the manufacturers guidelines. The sensors were installed at the locations where tag readers had been installed in order to be able to make a comparative analysis between different arterial travel time estimation systems. This resulted in vehicles going over the detector at fast and slow speeds, and even resting on top of them while waiting for the vehicles on the queue to move. Normally sensor arrays are installed just after the intersection to maximize free flow.

There was a winter storm with heavy snowfall that ended one day before the analysis period. This resulted in difficult driving conditions that are not typically encountered at many installation sites. The snow on the street blocked part of the bus lane along the segment due to snow being plowed to the side of the street, which resulted in vehicles (e.g. taxis) stopping or double parking in the slow lane. This led to considerable lane changing from the slow to the fast lane and to vehicles traveling off the center of the lane. These conditions are similar to the conditions described in [1] for on-ramps, for which the *modified method* improved performance.

A. Vehicle Detection System

The vehicle detection system deployed at the New York test site and used for this study was developed by Sensys Networks, Inc. This system consists of two access points and 20 wireless magnetic sensors installed in a five sensor array configuration in the middle of the fast and slow lanes at the start and end location, as shown in Figure 2. See [3] for details on this vehicle detection system.

Fig. 2. (a) Segment Start Location (b) Segment End Location

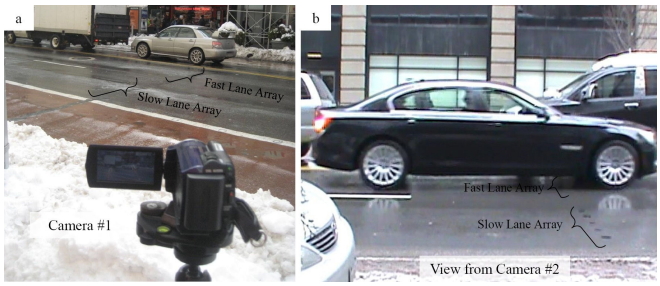

Fig. 3. (a) Camera recording vehicles at the START Location. (b) Camera recording vehicles at the END location.

TABLE I
VEHICLE COUNT BASED ON GROUND TRUTH AND SENSOR ARRAYS DATA

START location			END location		
	GT	Array		GT	Array
N^{fast}	205	214	M^{fast}	334	324
N^{slow}	290	292	M^{slow}	100	220
N	495	506	M	434	544

TABLE II
CHOSEN VEHICLES

k	l	*Veh. Type*	*Lane : Start* $\rightarrow$ *End*	*Travel Time* [*sec*]
11	τ	Taxi, car	–	–
12	τ	SUV	–	–
13	11	Taxi, car	$fast \rightarrow fast$	49
14	12	SUV	$fast \rightarrow slow$	50
15	18	Car	$fast \rightarrow fast$	107
16	τ	Taxi, prius	–	–
17	τ	Car	–	–
18	19	Bus	$slow \rightarrow fast$	116
19	τ	Car	–	–
20	20	Taxi, car	$slow \rightarrow fast$	116
21	21	SUV	$fast \rightarrow slow$	116
22	22	Taxi, minivan	$fast \rightarrow fast$	115
23	24	Bus	$slow \rightarrow fast$	121
24	26	Car	$slow \rightarrow fast$	120
25	τ	Minivan	–	–

IV. DATA

A. Ground Truth Data

Ground Truth (GT) data was obtained from videos recorded on January 28, 2011 from 10:54 am to 11:41 am. A time stamp, transited lane, vehicle type, and the vehicle position with respect to the middle of the lane were recorded for each vehicle entering or leaving the arterial segment at the start and end locations.

Two independent cameras were used to obtain the ground truth data. From the first camera (Figure 3 (a)) it was possible to obtain the time $s^{lane}_{GT_k}$ when vehicle k entered the arterial segment at the start location and went across the sensor array located on either the *fast* or the *slow* lane, where $s^{lane}_{GT_1} \leq s^{lane}_{GT_2} \leq \cdots s^{lane}_{GT_{N_{GT}}}$. From the second camera (Figure 3 (b)) it was possible to get the time $t^{lane}_{GT_l}$ when vehicle l exited the arterial segment and went through the downstream array located on either the *fast* or the *slow* lane, where $t^{lane}_{GT_1} \leq t^{lane}_{GT_2} \leq \cdots t^{lane}_{GT_{M_{GT}}}$. The data used to obtain a GT travel time distribution consists of two vectors $\{s^{lane}_{GT_k}, k = 1, \cdots, N_{GT} = 495\}$ and $\{t^{lane}_{GT_l}, l = 1, \cdots, M_{GT} = 434\}$.

The GT matching of upstream to downstream vehicles $k \rightarrow l$ was done visually and resulted in 318 matches. 177 entering vehicles k did not have a matching exiting vehicle l (e.g. vehicles turned or parked before reaching the end location) while 117 exiting vehicles l were not matched to any entering vehicle k (e.g. vehicles got into the segment at an intersection or were originally parked inside of it).

B. Vehicle Detection System Data

Consider a link formed by one of the start arrays, *laneS*, and one of the end arrays, *laneE*. During the video recording time interval, detection events indexed $i = 1, \cdots, N^{laneS}$ were registered by *laneS* at times $s^{laneS}_1 < s^{laneS}_2 < \cdots s^{laneS}_{N^{laneS}}$. This array measured a signature X^{laneS}_i each time there was a vehicle detection event i together with the time s^{laneS}_i. Detection events indexed $j = 1, \cdots, M^{laneE}$ were registered by *laneE* at times $t^{laneE}_1 < t^{laneE}_2 < \cdots t^{laneE}_{M^{laneE}}$. This array measured a signature Y^{laneE}_j each time there was a detection event j together with the time t^{laneE}_j. For this study, the vehicle detection system data consists of four arrays: (s^{slow}_i, X^{slow}_i) , (s^{fast}_i, X^{fast}_i), (t^{slow}_j, Y^{slow}_j) and (t^{fast}_j, Y^{fast}_j). Table I summarizes the vehicle detection system counts and compares them against the ground truth. Note that detection errors cannot be avoided and may create multiple signatures of the same vehicle at one location or may result on missing signatures due to undetected vehicles, as discussed in [4].

The vehicle re-identification algorithm summarized in Section II can be independently applied to the following combinations of data arrays: $fast \rightarrow fast$, $fast \rightarrow slow$, $slow \rightarrow fast$, and $slow \rightarrow slow$, even though traditionally only the first and the fourth combinations are used.

1) Subset of Vehicles: In order to be able to analyze the system performance in detail, a platoon of 15 continuous vehicles were chosen from the 495 vehicles that entered the arterial segment at the start location. These vehicles are shown in Table II. From this subset, a few vehicles were chosen to analyze their vehicle signatures.

V. Ground Truth and Vehicle Detection System Data Analysis

A. Lane Changing

Lane changing can have a significant degrading effect on the travel time estimation system performance if it continuously occurs as vehicles are going over the sensor arrays. If vehicles are traveling evenly in between lanes as they are going through the start or end location, the signature is split between both arrays at that location, and the middle part of the signature, which is generally the most useful, is not correctly measured by any of them. When this happens vehicles are very likely to be unmatched by the algorithm, reducing the vehicle re-identification rate.

Lane changing was very common during the analysis period. The main reason why people where changing lanes at the arterial segment was to overtake vehicles obstructing the slow lane. A large portion of the vehicles that changed lanes close to the end location triggered a detection event at both the fast and slow sensor arrays. This is reflected in the data from Table IV, that shows that 122 vehicles that entered the segment through the slow lane, exited it through the fast lane, while only 22 vehicles entered in the fast lane and exited in the slow one. Furthermore, Table I shows an overall 25% vehicle counting error by the vehicle detection system at the end location, while counting error in the start location was only 2.3% .

The large discrepancy in vehicle counting and the continuous lane changing were the result of vehicles double parked for extended periods of time in the slow lane downstream of the end location. This forced vehicles on the slow lane to change to the fast lane as they were exiting the segment. Many of these vehicles were almost completely changed to the fast lane as they were going over the end location, but some of the sensors from the slow array were also triggered by them. The exiting signatures of vehicles k = 15, 18 and 23 listed in Table II were some of the signatures studied because they were detected by both arrays as they were exiting the segment. Signatures from the slow lane array under this condition contained no useful data; most of the vehicle signature information was captured in the signature data measured by the fast lane array. After this analysis it was observed that when a vehicle triggers detection events at multiple arrays at the same location while going mostly in one lane, significant vehicle counting error in one of the lanes may result. However, this would barely affect the travel time estimation results because signatures coming from the unused lane array would yield large distances in the signal processing step of the vehicle re-identification algorithm (see Section II) which would make them unmatched.

B. First In, First Out Condition

As it was mentioned in Section II, the matching algorithm is constrained and does not allow overtaking. In other words, when the matching step is performed, the sequence of matched vehicles satisfies the FIFO condition. With the ground truth data collected from video it is possible to determine the effect of the FIFO constraint on the matching rate upper bound. Note that since the vehicle re-identification algorithm is run independently for different array combinations, the FIFO constraint is only imposed among vehicles going on the same link.

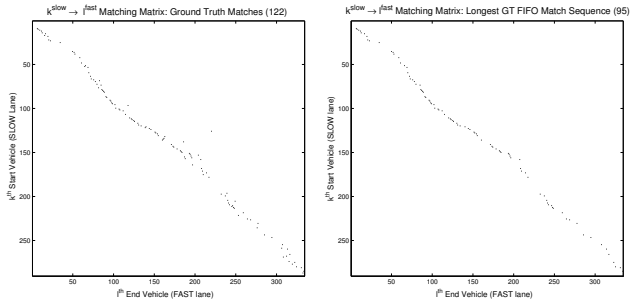

Fig. 4. Synthetic Distance Matrix (left) Complete Data Set (right) Largest Vehicle Sequence Satisfying the FIFO condition

Figure 4 (left) is the gray scale coding of a matrix that relates the start signatures measured by the slow lane array to the end signatures measured by the fast lane array (i.e. link $slow \rightarrow fast$) based on GT data. If the k^{th} signature (row) and the l^{th} signature (column) correspond to the same vehicle, the pixel is black, otherwise it is white. A perfect matching algorithm would re-identify 122 vehicles across this link. However, if a FIFO constrained vehicle re-identification algorithm is used instead, it would be possible to match only 95 vehicles, which corresponds to the number of elements in the largest vehicle sequence, out of the 122 vehicles, that satisfy the FIFO constraint. Figure 4 (right) shows the gray scale coding of the matrix with this vehicle sequence. For this particular link, 72 % is the upper bound on the matching rate that could be expected from the re-identification algorithm summarized in Section II assuming perfect accuracy.

Table IV lists, in the second and third column, the number of vehicles that went across each of the links in the arterial segment. In the fourth and fifth column this table lists the maximum number of vehicles that satisfy the FIFO constraint in each of the links, which correspond to the upper bound on the number of re-identified vehicles for a FIFO constrained matching algorithm. From this table it can be seen that out of the 318 vehicles that crossed the segment, only 270 could be matched by the vehicle re-identification algorithm if perfect performance is assumed, which accounts for 85 % of the vehicles.

The FIFO constraint improves accuracy of the system, as mentioned in [2], without significantly reducing the maximum possible number of matches.

C. Travel Time by Vehicle Category

The travel time distribution estimates are affected by the FIFO constraint. If there is a particular vehicle group with significant presence along the arterial segment under consideration, and a large percentage of the vehicles in the

group violates the FIFO condition as they go across, then discrepancies between the ground truth and the estimated travel time distributions should be expected.

The algorithm would be able to predict accurately the travel time information of vehicles that want to go across the segment without stoping, since it is assumed that these are the majority of the vehicles and for the most part follow the FIFO condition. Taxis or buses are vehicle groups that have a tendency to stop and end up violating the FIFO constraint. If the percentage of vehicles in these groups is large with respect to the total number of vehicles going across the segment, and if there are considerable bus routes with multiple stops and common locations for taxis to drop off and pick up passengers, then the travel time distribution based on the ground truth data will be significantly different from the estimated one. Nevertheless, as far as a traffic agency and drivers that rely on travel time estimation are concerned, this should not represent a problem, since the information that can be extracted from the estimated travel time distribution would be useful and representative of the traffic conditions at the arterial segment under consideration.

Table III lists the different types of vehicles and the number of them that entered the segment at the start location, exited through the end location and went across it. The Table also lists information about the travel time distribution divided by vehicle type. For the most part, all the vehicles have similar travel time characteristics. For the test site in New York City, taxi presence is significant, accounting for 30.5 % of the vehicles that went across the segment. Note that their travel time distribution's 25th percentile, median and 75th percentile are very close to those of the total distribution. The buses' travel time distribution has the larger 25th percentile, median and 75th percentile, which is expected, since there are several bus stops along the segment. Since buses only represent 5.3 % of the total number of vehicles that crossed the segment, their influence is not significant. Figure 5 (top) shows the travel time distributions based on GT data for taxis and buses while Figure 5 (bottom) shows the travel time distribution of all the vehicles except taxis and buses. Note that both distributions look similar with almost the same median, but a larger difference at the 90th percentile, which is the result of long travel times corresponding mainly to buses. The travel time distribution of taxis and buses, across the test site and during the analysis period, seems to reflect street traffic conditions.

Based on the results from this section, an accurate travel time distribution based on the matching algorithm described in Section II should be similar to the one obtained based on the ground truth data. Slightly lower percentiles in comparison to the GT distribution are expected due to outliers and travel times from vehicles not satisfying the FIFO condition with travel times in between the 50 and 100 seconds (e.g. taxis making short stops but not stopping at any red light).

TABLE III
GROUND TRUTH DATA BY VEHICLE TYPE

Vehicle Type	Start Counts	End Counts	GT Matched	25th Perc	Median TT [sec]	75th Perc
bicycle	2	4	1	126	126	126
bus	30	22	17	60	106	142
car	111	101	75	51	100	116
minivan	23	20	14	52	87	115
pick up	13	7	6	64	87	107
SUV	93	86	60	50	80	109
taxi	160	123	97	50	94	115
truck	32	36	25	58	103	117
van	21	35	23	50	66	110
TOTAL	495	434	318	51	98	115

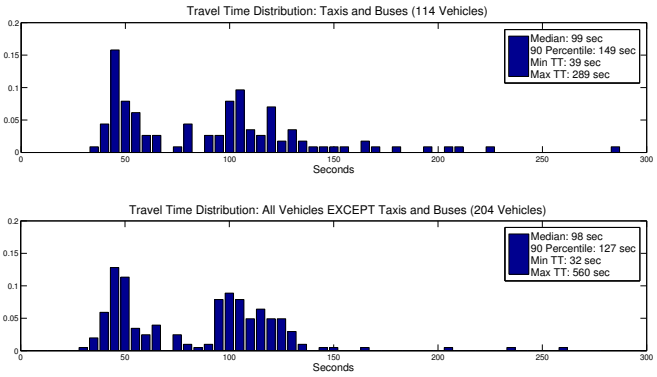

Fig. 5. Travel Time Frequency Distribution by Vehicle Type (top) Taxis and Buses. (bottom) All Vehicles except Taxis and Buses.

VI. TRAVEL TIME RESULTS

In this section the GT travel time distribution is compared to the travel time distributions computed with the *original method* and the *modified method*.

Table IV shows the results obtained from the vehicle re-identification algorithm for the *original method* and the *modified method*. The total number of matched vehicles for each method is listed as well as the number of re-identified vehicles per link (e.g. $fast \rightarrow fast$, $fast \rightarrow slow$, $slow \rightarrow fast$ and $slow \rightarrow slow$). Traditionally only $fast \rightarrow fast$ and $slow \rightarrow slow$ links are used, since it is assumed that most vehicles stay in the same lane as they go through an arterial street. However, the GT data shows that 122 vehicles that entered the segment through the slow lane exited through the fast lane, which accounts for 38% of the vehicles that crossed the arterial segment. For this reason it was decided to use the four links to estimate vehicle travel times. As it can be seen from Table IV, for both of the methods, the

TABLE IV
MATCHING RESULTS COMPARISON

	Ground Truth		GT (FIFO)		Original Method		Modified Method	
Start\End	*Fast*	*Slow*	*Fast*	*Slow*	*Fast*	*Slow*	*Fast*	*Slow*
Fast	129	22	119	19	62	19	77	17
Slow	122	45	95	37	66	51	78	49
Total	318		270		198		221	

number of matched vehicles obtained using the $slow \rightarrow fast$ link accounts for a large percentage of the number of re-identified vehicles. The $fast \rightarrow slow$ link is not as important, but it increases the matching rate for both methods.

The vehicle re-identification rate for the *original method* is 62%, while for the *modified method* it is 69%. Table IV (columns 4 and 5) shows the vehicle re-identification upper bound for each of the links. Note that a considerable percentage of the matched vehicles in the $slow \rightarrow slow$ link is expected to be inaccurate for both estimation methods, since the number of matched vehicles exceeds the upper bound based on the FIFO constraint. The *original method* overestimates the number of matched vehicles by at least 14, while the *modified method* does it by 12. At least 7% of total travel time estimates calculated with the *original method* are inaccurate while at least 5 % are inaccurate for the *modified method* results.

Figure 6 compares the *original method* travel time distributions against the GT. The *original method* estimated distribution seems to capture the GT distribution at short travel time values. However, the number of estimated travel times above 150 seconds exceeds the ones observed in the GT data. This suggests that some of these long travel times were calculated from X_i, Y_j vehicle signature pairs that were incorrectly matched. Figure 7 shows that the GT and the *original method* cumulative distribution functions (CDF) correlate well at short travel times, but start diverging right after the median, reaching an error of 17% at the 75th percentile and 52% at the 90th percentile.

Figure 6 compares the *modified method* travel time distributions against the GT. The *modified method* travel time distribution correlates well with the GT data. Figure 7 shows that the GT and the *modified method* cumulative distribution functions (CDF) have a similar shape. The estimated CDF is shifted to the left of the GT CDF, with a maximum error of 17% close to the median. The error between both CDFs is very small right after the 65th percentile, with a 3.5% error at the 75th percentile and 2.3% error at the 90th percentile. The differences observed between the GT and the estimated travel time distributions with the *modified method* correspond to the differences expected in Section V for an accurate FIFO constrained matching algorithm at the test site.

VII. CONCLUSION

A vehicle travel time estimation system was studied on an arterial segment in New York City using ground truth data collected from video. The ground truth data was valuable to understand the traffic phenomena that occur at arterial streets like lane changing, vehicle overtaking, vehicles traveling in between lanes, among others, which directly relate to the performance of the travel time estimation system. It was possible to apply the vehicle re-identification algorithm using sensor array data from different lanes, $fast \rightarrow slow$ and $slow \rightarrow fast$, something that has not been tried before with this system and that led to an increase on the vehicle re-identification rate. Furthermore, it was shown that the

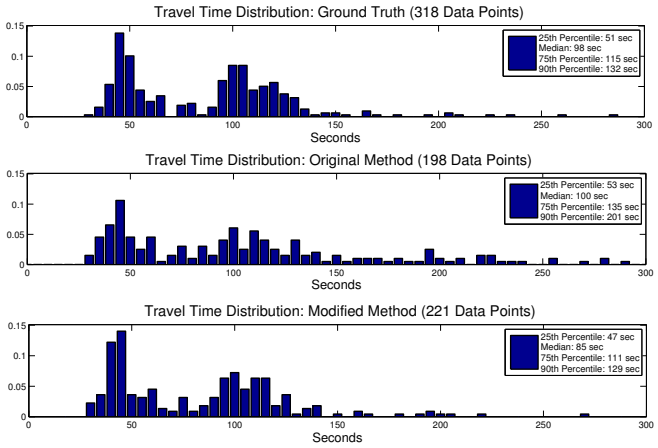

Fig. 6. Travel Time frequency distribution for the ground truth, the original method and the modified method

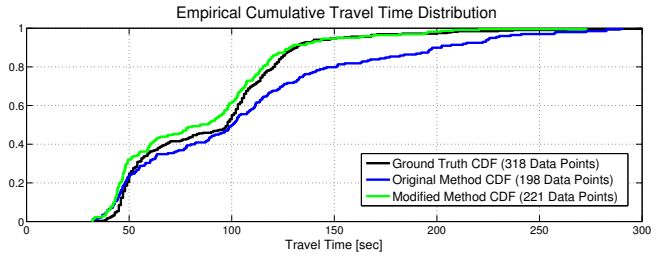

Fig. 7. Empirical Cumulative Travel Time Distribution for the GT, Original Method and Modified Method

FIFO assumption that constrains the matching algorithm is adequate at arterial implementations. The matching rate for the *original method* was 62% while that of the *modified method* was 69%. Even though there is not a big difference in the matching rate, it seems that the *modified method* is more accurate, since its travel time distribution and cumulative distribution function are closely related to the ground truth ones. The *original method* travel time CDF does not match the GT, especially at long travel times, while the *modified method* has an improved performance in this aspect. At the 75th percentile, the original method error is around 17%, while the *modified method* error is less than 3.5%.

REFERENCES

[1] R. O. Sanchez, C. Flores, R. Horowitz, R. Rajagopal, and P. Varaiya. "Vehicle Re-Identification Using Wireless Magnetic Sensors: Algorithm Revision, Modifications and Performance Analysis," in *Proceedings of the IEEE International Conference on Vehicular Electronics and Safety*, Beijing, China, July 2011.

[2] K. Kwong, R. Kavaler, R. Rajagopal, and P. Varaiya. "Arterial travel time estimation based on vehicle re-identification using wireless magnetic sensors," in *Trans. Res. Part C: Emerging Technol.*, vol. 17, no. 6, pp. 586-606, 2009.

[3] A. Haoui, R. Kavaler, and P. Varaiya, "Wireless magnetic sensors for traffic surveillance," in *Transp. Res. Part C: Emerging Technol.*, vol. 16, no. 3, pp. 294-306, 2008.

[4] R. O. Sanchez, R. Horowitz, and P. Varaiya, "Analysis of queue estimation methods using wireless magnetic sensors," accepted for publication at the *Trans. Res. Rec., Journal of the Transportation Research Board*, 2011.